Sajad Namdari[1]; Alireza Baghbanan[1]; Hamid Hashemolhosseini[2]

[1] *Department of Mining Engineering, Isfahan University of Technology, Isfahan 8415683111, Iran*

[2] *Department of Civil Engineering, Isfahan University of Technology, Isfahan 8415683111, Iran*

Abstract

Understanding the fluid behaviour in rock masses is of great importance in various rock mass-related engineering projects, such as seepage in tunnels, geothermal reservoirs, and hazardous waste disposal. Different approaches have been implemented to study the flow pattern in fractured porous rock masses. Laboratory experiments can provide good information regarding this issue, but high expenses aside, they are time-consuming and suffer the lack of ability to study field scale mediums. Numerical methods are beneficial in simulating such mediums with the Discrete Fracture Network (DFN) method in terms of costs and time as they offer sufficient flexibility and creativity. In this paper, a Matlab code was extended to study the flow regime in a Dual Permeability Media (DPM) with two point sources in the right and left side of the model as an injector and a producer well, respectively. A high permeability discontinuity with different angles was embedded in a very low-permeability limestone matrix. Pressure equations were solved implicitly with a two-point flux approximation scheme of the Finite Volume Method (FVM). Streamlines were traced in the medium and used to analyse the model's hydraulic behaviour with the aid of Time Of Flight (TOF) for each point. The results show that the FVM-DFN hybrid method can be used as a fast method for fluid flow in DPM with the aid of streamline simulation to study the fluid flow in a large model with discontinuity.

1. Introduction

Different types of discontinuities, such as bedding planes, joints, fractures and faults are present in the upper layer of the Earth's crust. Such discontinuities form a complex system that makes significant changes, not only in the mechanical behaviour of the rock mass, but in its hydraulic behaviour as well.

Many problems in today's rock engineering demand a better understanding of the flow process in rock masses. Fluid flow can affect both the hydraulic and mechanical properties of a medium. In many studies, a rock mass consists of an impermeable matrix, which cannot conduct fluids, and a system of fractures is the only channel for fluid to flow through. In many cases of rock mechanics problems, the assumption of an impermeable rock matrix will interrupt the precision of the simulation output. Some previous studies have pointed out that the effective porosity and permeability of a matrix, even at very low magnitudes, can change the flow regime and hydraulic behaviour of a system (**Odling and Roden, 1997; Zhang and Sanderson, 2002; Namdari et al.,**

2012; Habibi et al., 2014; Namdari et al., 2016; Olu-Ojo, 2020). In underground mining and tunnelling in porous rocks, fluid flow can play a significant role in both designing and implementing the designed outline. In geothermal reservoirs, the fluid should circulate properly in the hot zones of interest. Without good insight into the fractured rock mass flow pattern and geometry, it would be impossible to implement the project with the desired efficiency (**Macenić et al., 2018**). In petroleum engineering, an essential issue is to know and predict the movement of crude oil, gas, and saline water in both fractures and matrix. Due to the change of the mechanical properties, the ground's hydraulic properties can strongly defect the underground openings' stability and, therefore, change the mining method (**Ooriad et al., 2018**). Also, in deep drilling operations, any medium-sized to large fracture or fault can suspend the drilling process due to mud loss, and thus the progression of the whole project will slow down. In wellbore stability, one of the main issues is the flow of the drilling mud and the water in the ground-drilling system (**Pašić et al., 2007**). Even in the prediction of pollution migration in underground water, the results are highly dependent on the behaviour of the underground water, which is mainly controlled and dominated by the fracture system and

Corresponding author: Alireza Baghbanan

bagh110@iut.ac.ir

overall permeability of the medium (**Ružičić et al., 2012**). It is clear that understanding the fluids and their behaviour in fractured rock masses, particularly on a large scale, is of great importance in various fields of rock engineering.

Analytical and numerical methods have been developed and used extensively to deal with this subject. Although analytical techniques can provide helpful insight into the flow mechanisms, they are restricted to simple geometry and demand a vast knowledge of advanced mathematics for a more complex fractured medium (**Namdari et al., 2016; Wang et al., 2019**). On the other hand, numerical methods are flexible in terms of implementation and can be utilized in almost any complex geometry (**Seales, 2020**).

As a consequence of the importance of this issue, hundreds of research papers have addressed this subject through the last century to this present year. **Bear et al., (1993)** published a book on flow and contaminant transport in fractured rock. **Odling and Roden (1997)** simulated the contaminant transport in fractured rock with significant matrix permeability with En-Echelon natural fracture system using Finite Difference Method (FDM). **Zhang and Sanderson (2002)** modelled a small Dual Porosity-Dual Permeability Model (DPM) with 3 parallel fractures under stress. They showed that increasing the maximum principal stress can hugely affect the overall image of flow. Trends, prospects, and challenges in quantifying flow and transport through fractured rocks were studied by **Neuman (2005)** and it was reported that the main challenge is to quantify the exchange of fluid between fracture system and matrix, which is defined through transfer functions. **Baghbanan and Jing (2007)** investigated the hydraulic properties of fractured rock masses with correlated fracture length and aperture. Their research paper showed that a suitable ellipse of anisotropic permeability could be reached only in cases with relatively large dimensions compared to the fracture medium length.

With significant advances in computing capacities over the years, numerical methods were used frequently by the authors. **Namdari et al., (2012)** contracted a comparison between a model without matrix permeability and a model with a very low-permeability matrix with simulating over 1800 realization models through the Monte-Carlo simulation technique. It was shown that even in low magnitudes, matrix permeability can change the whole flow regime and overall permeability of a medium. **Siavashi et al., (2014)** developed a 3D streamline-based simulation of two-phase flow in heterogeneous porous media. The speed of this method was reported to be much higher than other peer methods in heterogeneous media simulation. In 2015, a streamline tracing algorithm in heterogeneous porous rock to predict Time Of Flight (TOF) and breakthrough curves was studied by **Nunes et al (2015)**.

The equivalent Discrete Fracture Network (DFN) for highly fractured rock mass was reported in the study of **Ren et al (2017)**. They simplified the highly fractured rock to a sparser system of fractures, which decreases the amount of time needed to simulate a model. In 2019, **Zhang et al** investigated the complexities of the hydraulic fracturing process in naturally fractured rock masses. The Synthetic Rock Mass (SRM) method was used and extended through the combination of the Discrete Element Method (DEM) and the Discrete Fracture Network (DFN) to assess the uncertainties. In 2020, **Wang et al.** performed a tracer test and streamline simulation for geothermal resources in Cuona of Tibet to measure the impact of injection wells in the production of sink wells in different well patterns of this geothermal reservoir. A streamline simulation of experimental studies on water-flooding under given pressure boundaries was conducted as a coupled Hydro-Mechanical (HM) process by **Zhang et al. (2021)**. With the help of the streamline simulation, the capillary effects at the fluid front were quantified as a function of time and coordinates.

One of the key concepts to address here is that discontinuous rock masses do not behave as a continuum (**Namdari et al., 2016; Sun et al., 2020**). The simulation process of fluid flow in fractured rock masses should deal with discontinuities on a large scale. The most used numerical method to study the fluid flow in the fractured discontinuum medium is Discrete Fracture Network (DFN) (**Jing and Stephansson, 2007; Baghbanan, 2008; Habibi et al., 2014; Karimzadeet al., 2017; Baghbanan et al., 2019; Li et al., 2020; Huang et al., 2021a**). It is an appropriate method when dealing with impermeable rock matrix and delivers good speed and accurate results (**Habibi et al. 2014**). The speed of this method will drop drastically by applying the permeable matrix to the model (**Namdari et al., 2012; Namdari et al., 2016**). It takes days or weeks to run a single realization for a desired dual permeability medium (**Namdari et al., 2012; Habibi et al., 2014; Namdari et al., 2016**). Furthermore, the Monte-Carlo simulation, which is a widely accepted and applied technique and has been used in many studies, demands numerous numerical simulations on different realizations (**Jing and Stephansson, 2007; Namdari et al., 2012; Habibi et al., 2014; Huang et al., 2021b**). The number of realizations needed to study different hydraulic parameters can reach hundreds or even thousands models (**Namdari et al., 2012; Habibi et al., 2014**). Hence, the desired method to treat this issue should be fast enough to be able to simulate numerous models in a limited amount of time. In this case, streamline simulation is a scientifically approved method to investigate the hydraulic behaviour of a heterogeneous medium (**Thiele, 2002; Datta-Gupta and King, 2007; Nunes et al., 2015; Dailami et al., 2020; Wang et al., 2020**). In this method, the 3D or 2D equations are broken into 1D equations along some curves called streamlines, which makes this method 2 or even 3 orders of magni-
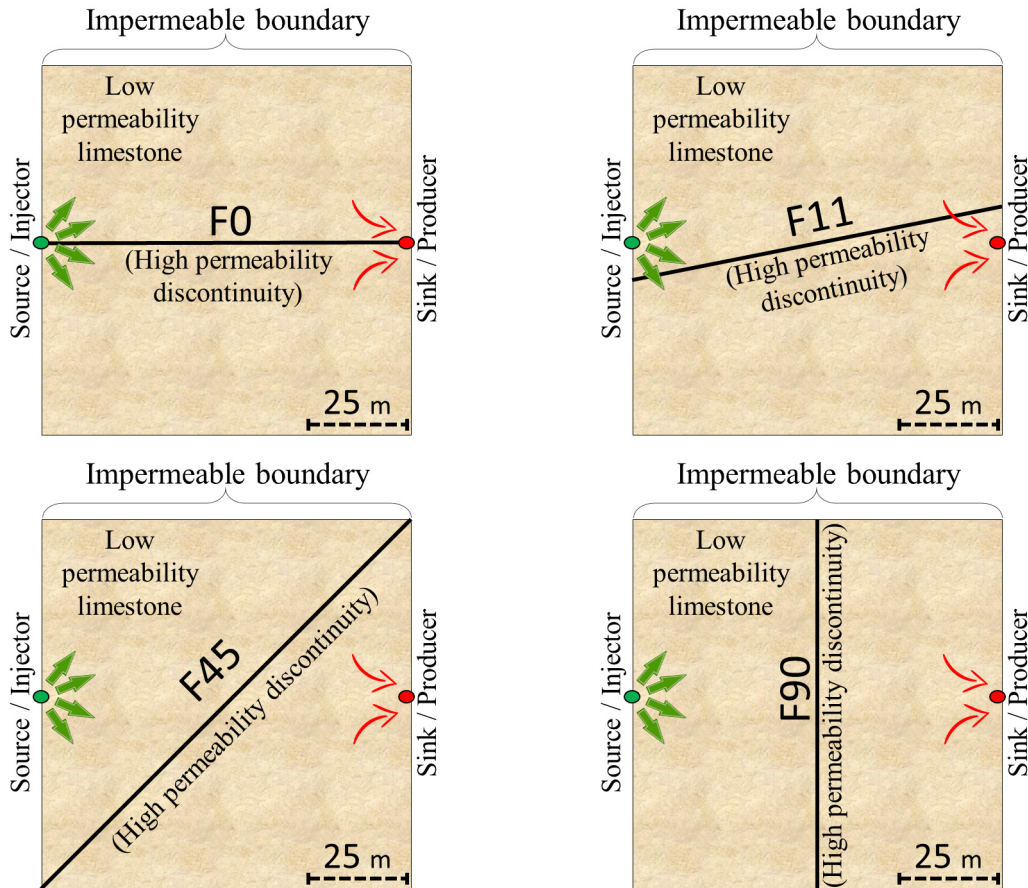
Figure 1: Schematic presentation of a low permeability matrix with high permeability discontinuity in different angles of 0, 11, 45, and 90 degrees represented with the names *F0, F11, F45* and *F90* respectively. All boundaries are defined as impermeable.

tude faster, compared to discrete methods (**Datta-Gupta and King, 2007**; **Zhang et al., 2021**).

In this study, the effect of a large discontinuity with different angles in a low permeability limestone matrix is investigated in a 2D square of 100×100 m², which is constructed with 2500 cells in the Cartesian coordinate system. To research the discontinuity effect on pressure and flow paths of fluid, the direction angle of the discontinuity is changed from 0 to 11, 45 and 90 degrees with respect to the X-axis. The low permeability rock mass cells are replaced with high permeability cells representing the discontinuity. Through this approach, the main model consists of two main parts: rock matrix cells, which have low porosity and low permeability, and discontinuity cells with a relatively higher porosity and very high permeability. Within this approach, the discontinuity, which is a line, will be replaced by some consecutive porous and high permeability cells in the same direction as the original discontinuity. The newly employed approach in this paper is to use a hybrid approach of the Finite Volume Method (FVM) and the Discrete Fracture Network (DFN), namely FVM-DFN to form a cell-based method. Streamline simulation is used afterwards to trace the path of fluid particles to give a more

detailed vision into the flow mechanisms in a fractured porous media, which is lacking in the previous studies, particularly in the rock mechanics research area. Resulting from this, besides the improvement of runtime (which has been decreased to less than one minute for each simulation, in contrast to DFN-DEM approach with hours of simulation time), the amount of time will not increase even for a large number of discontinuities, because the number of equations to solve will not increase, and the cell numbers remain equal even with a high number of discontinuities through this approach. Moreover, this method provides some additional information against DFN methods. A streamline's path and Time Of Flight (TOF) contours will yield a more detailed insight into the hydraulic behaviour of a discrete model, which are missing in DFN methods. In addition, stagnant regions and the overall flow paths will be obtained as opposed to discrete methods.

2. Methods

In this section, the description of the model is presented. The basic concepts of the finite volume method (FVM) and the Two-Point-Flux-Approximation ap-

proach (TPFA) are presented. The streamline tracing method is discussed afterwards.

2.1. Model description

In real subsurface conditions, discontinuities tend to have irregular shapes with generally rough surfaces. Also, sedimentary rocks are not homogenous and isotropic due to the layering nature of these rocks and the stress path during the consolidation process. To study the subsurface flow phenomenon, some simplifications may be applied due to the complex behaviour of the ground. Some widely applied simplifications are the assumption of an isotropic rock matrix and representation of discontinuities with a straight line, which is used in DFN approaches (**Jing and Stephansson, 2007**).

The models consist of a 2D horizontal 100×100 m² square with a large discontinuity and impermeable boundary. The rock matrix is a compacted low permeability isotropic limestone. Two source and sink points exist in the middle left and right edge of the square. The discontinuity exists in the square with four different angles of 0, 11, 45, and 90 with respect to the X-axis with the names *F0*, *F11*, *F45*, and *F90* (see **Figure 1**).

In this study, the rock matrix assumed to be a homogeneous and isotropic low permeability limestone. The boundaries cannot permeate the fluid and are defined as impermeable. Hence, the only source and sink points of the model are injector and producer points. Moreover, it is assumed that the discontinuities are a completely straight and homogeneous porous material with very high permeability compared to rock matrix permeability. The matrix's effective porosity is equal to 5% with 0.1 mD (millidarcies) permeability, while the discontinuities are defined as a porous medium with 20% porosity and a permeability of 800 mD. This scheme aims to investigate the effect of different directions of discontinuity with high permeability in a large scale in the absence of gravity and body forces.

2.2. Finite Volume Method (FVM) and Two-Point Flux Approximation approach (TPFA)

In the FVM, the basic mathematical idea is to convert volume integrals in a partial differential equation that contains a divergence to surface integrals, using the divergence theorem (**Sokolova et al., 2019**). Fluxes at the surfaces of each Finite Volume will be derived afterward. These terms are then evaluated as fluxes at the surfaces of each finite volume. Since an incompressible fluid entering a given volume is identical to that leaving the adjacent volume, these methods are conservative. The technique is used in many computational fluid dynamics packages (**Moukalled et al., 2016**). Finite volume refers to the small volume surrounding each node point on a mesh. Due to the physical concept of FVM, it is a more robust method compared to FEM and FDM in the context of fluid flow.

In FVM, the basic assumption is the physical concept of conservation of mass, or for an incompressible fluid, conservation of volume. In this study, it was assumed that there is a single-phase fluid in the model. Hence, it can be written:

$$\nabla \cdot \vec{v} = q, \vec{v} = -K\nabla p (\Omega \subset R^d) \qquad (1)$$

Where:

v – Velocity vector (m/s)

q – Flow rate (m³/s)

K – Hydraulic conductivity (m/s)

p – Pressure head (m)

Rewriting Equation 1 will yield the integral form:

$$v_{i,k} = \int_{\Gamma_{i,k}} \vec{v} \cdot \vec{n} \ ds \quad , \ \Gamma_{i,k} = \partial\Omega_i \bigcap \partial\Omega_k \qquad (2)$$

Where:

n – Normal vector on the surface of the control volume

To develop a finite volume discretization, rewriting Equation 2 in integral form using a single cell i in the discrete grid and then applying the midpoint rule to calculate the integral will yield:

$$v_{i,k} \approx A_{i,k}\vec{v}\left(\vec{x}_{i,k}\right) \cdot \vec{n}_{i,k} = -A_{i,k}\left(K\nabla p\right)\left(\vec{x}_{i,k}\right) \cdot \vec{n}_{i,k} \qquad (3)$$

Where $x_{i,k}$ is the centroid on $\Gamma_{i,k}$. **Figure 2** shows a schematic representation of two adjacent cells i and k in a Cartesian system.
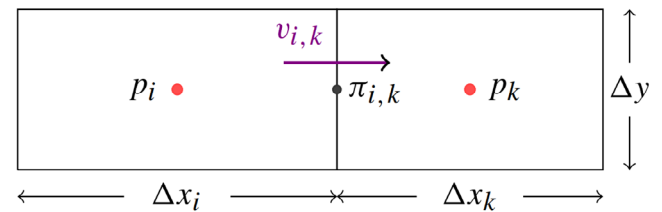

Figure 2: Two cells used to derive the TPFA discretization for a 2D Cartesian grid (**Lie, 2019**)

If it is assumed that the pressure gradient is linear inside each cell, it follows that (**Lie, 2019**)

$$v_{i,k} \approx A_{i,k}K_i \frac{\left(p_i - \pi_{i,k}\right)\vec{c}_{i,k}}{\left|\vec{c}_{i,k}\right|^2} \cdot \vec{n}_{i,k} = T_{i,k}\left(p_i - \pi_{i,k}\right) \qquad (4)$$

Where:

T – Transmissibility (m/s)

A – Area (m²)

$\pi_{i,k}$ – Pressure head at the face centroid (m)

The transmissibility is introduced here as T parameter. The continuity of fluxes yield that $v_{i,k} = -v_{k,i} = v_{ik}$ and for pressure $\pi_{i,k} = \pi_{k,i} = \pi_{ik}$. This leads to two equations below:

$$T_{i,k}^{-1}v_{ik} = p_i - \pi_{ik} \quad , \ -T_{k,i}^{-1}v_{ik} = p_k - \pi_{ik} \qquad (5)$$

By eliminating the interface pressure πik, it ends up with the following two-point-flux-approximation (TPFA) scheme

$$\vec{v}_{ik} = \left[T_{i,k}^{-1} + T_{k,i}^{-1} \right]^{-1} \left(p_i - p_k \right) = T_{ik} \left(p_i - p_k \right) \qquad (6)$$

Where *Tik* is the transmissibility associated with the connection between the two cells of *i* and *k*.

2.2. Streamline-based flow simulation

A streamline is a line that is tangential to the instantaneous velocity direction (velocity is a vector, and it has a magnitude and a direction). To visualize this in a flow, one can imagine the motion of a small marked element of fluid. Since the velocity at any point in the flow has a single value (the flow cannot go in more than one direction simultaneously), streamlines cannot cross (**Datta-Gupta and King, 2007; Chen et al., 2020**). A streamline is the path of fluid particles flowing from the injection well to the production well. It can be defined as the line that is made of points of equal streamline function values. At any time, the tangential direction of each streamline point is identical to the velocity vector.

The most notable study for efficient tracing of the streamlines was performed by Pollock (**Thiele and Batycky, 2006**). In Pollock's method, the total input and output flux to each boundary is calculated with Darcy's Law (**Batista, 2020**). With the fluxes being calculated, the scheme focuses on calculating the coordinates of the exit point of the streamline and after that, it computes the amount of time that it takes for a particle to travel along a streamline from the inlet point to the exit (see **Figure 3**).
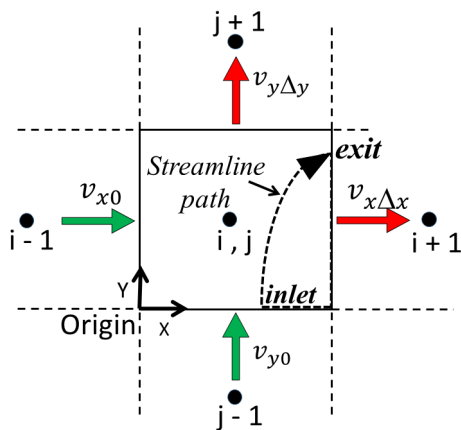

Figure 3: Pollock method for tracing streamlines in a Cartesian grid

The velocity in each direction (x or y in 2D) is calculated via a piece-wise linear approximation. If v is the interstitial velocity ($v = \nu/\varphi$), then a linear velocity approximation in the *x*-direction yields (and also the same for y):

$$v_x = v_{x0} + g_x (x - x_0) \;\; , \;\; g_x = \frac{v_{x\Delta x} - v_{x0}}{\Delta x} \qquad (7)$$

Where:

$v_x 0$ – Velocity in the *x*-direction $x = x_0$ (m/s)

g_x – Velocity gradient in the *x*-direction (1/s)

Since $v_x = \frac{dx}{dt}$, the exit time for each cell can be obtained by integration of the velocity in x-direction (and in the same way for y-direction) for each face for a known entry point (x_i, y_i) and exit point (x_e, y_e) and some simple algebraic manipulation:

$$\Delta t_x = \frac{1}{g_x} \ln \left[\frac{v_{x0} + g_x (x_e - x_0)}{v_{x0} + g_x (x_i - x_0)} \right],$$

$$\Delta t_y = \frac{1}{g_y} \ln \left[\frac{v_{y0} + g_y (y_e - y_0)}{v_{y0} + g_y (y_i - y_0)} \right] \qquad (8)$$

It is obvious that the streamline exits from the face with minimum travel time ($\Delta t_m = \text{MIN}\left(\Delta t_x, \Delta t_y \right)$), so the exit point coordinates are calculated by re-solving for x_e and y_e given the minimum time Δt_m:

$$x_e = \frac{1}{g_x} \ln \left[v_{xi} \exp \left(g_x \Delta t_m \right) - v_{x0} \right] + x_0,$$

$$y_e = \frac{1}{g_y} \ln \left[v_{yi} \exp \left(g_y \Delta t_m \right) - v_{y0} \right] + y_0 \qquad (9)$$

3. Results

In this section, simulation results for pressure contours, streamlines, and TOF contours are illustrated. Each simulation takes under 1 minute, which shows a drastic decrease in runtime for a model with dual permeability in both fracture and matrix (**Namdari et al., 2012 and 2016**).

3.1. Contours of pressure

It was noted in the previous sections that the boundaries are impermeable, and the fluid can only be injected or produced in the source and sink points. Pressure contours in the 4 cases are presented in **Figure 4.**

Pressure contours for the 4 cases are similar in shape and there is no sign of a difference in the shape of pressure distribution caused by different discontinuity angles. There is a significant issue to address here. The pressure distribution may almost be the same in shape, but the pressure magnitude is very different in each case. In the 0 degree angle, the pressure is smaller, practically by 2 orders of magnitude, compared to the three other cases. For the other three cases of *F11, F45* and *F90*, in which the injection is done in the low permeability matrix cell, the pressure range stays almost identical.
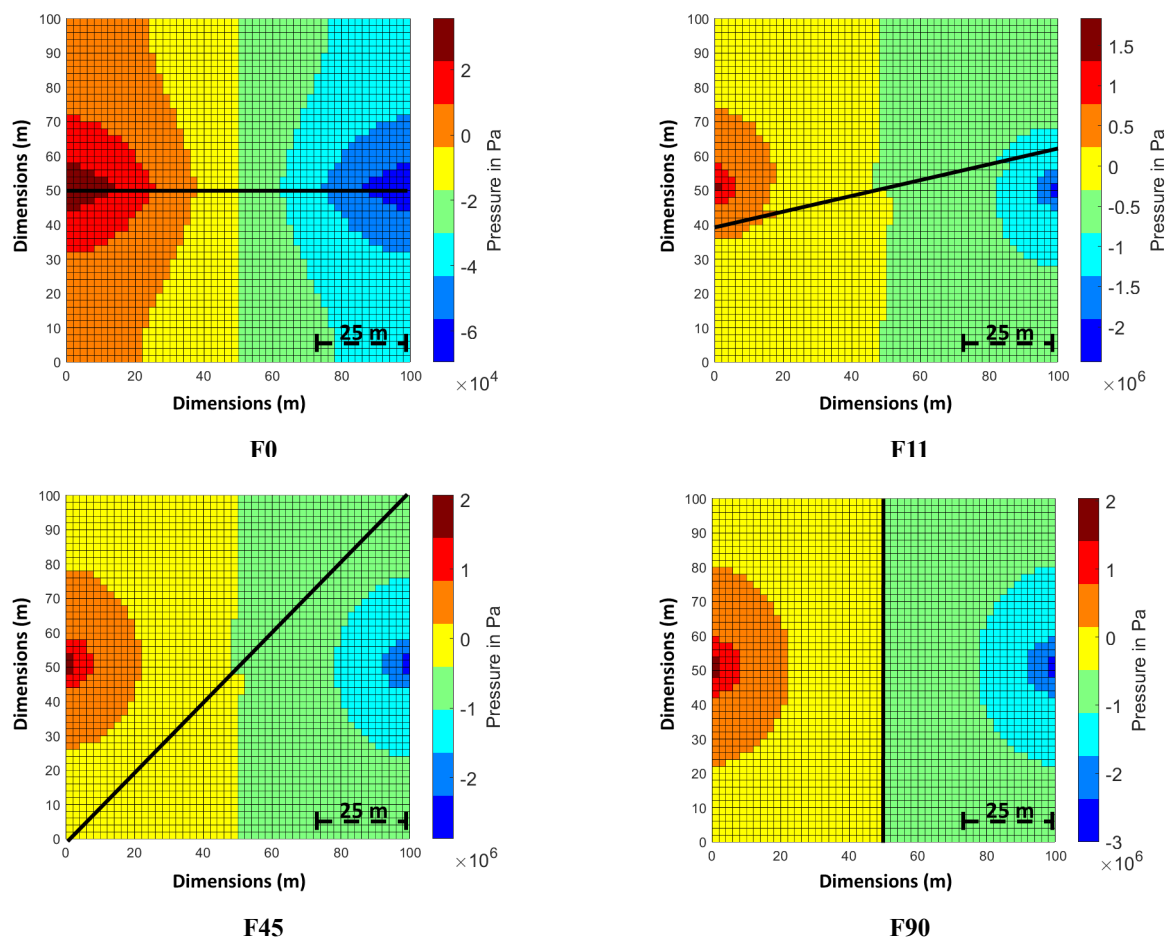
F0

F11

F45

F90

Figure 4: Pressure contours for each case. Solid lines represent discontinuity position in the model.

3.2 Streamlines

In **Figure 5**, generated streamlines for each case are shown. Discontinuity is drawn with a solid black line. In some cases, such as *F0* and *F11*, streamline concentration on the discontinuity is very high, showing a high permeability effect of the discontinuity. The high concentration of streamlines in these cases represents the high flow region in these two *F0* and *F11* discontinuities. In the *F45* case, streamlines change their direction, align with the discontinuity and then shift back to their original paths. However, the amount of change in this case is smaller in comparison to *F0* and *F11*.

In the *F90* case, streamlines don't show any change in the direction and there are no signs of any change in the streamlines path due to the existence of discontinuity.

3.3 Time of flight (TOF)

Time of flight contours are illustrated in **Figure 6**. The direction of the discontinuity has a considerable impact on the TOF contours.

For *F0*, the fluid flows very fast on the discontinuity line, and it takes the maximum amount of time for the

fluid to access other points on the matrix. It can be seen that the high permeability on the line segment between the source and sink is a preferred channel for fluid flow. The TOF contours show that other than cells on the discontinuity line in the *F0* model, TOF magnitudes for other cells in the model are about one order of magnitude higher than the same magnitude for *F11* and *F45* and two orders of magnitudes higher than the *F90*. Stagnant regions are formed in the upper and lower left of the *F0* model, which are presented with a red colour. In *F11*, the results resemble the *F0* model, with high TOF contours in the upper and lower left corners of the model. The smallest stagnant regions belong to the *F45* model, with more uniform contours. In *F90*, the high TOF contours are formed in the right half of the model.

In contour images, the stagnant regions are more important than the absolute magnitudes of TOF for each cell (**Lie, 2019**). This is because the contours represent the stagnant regions. If the medium is supposed to be saturated with fluid, the injection and production will be on a steady state cycle, so the absolute value for TOF will be in the second order of importance.

F0

F11

F45

F90
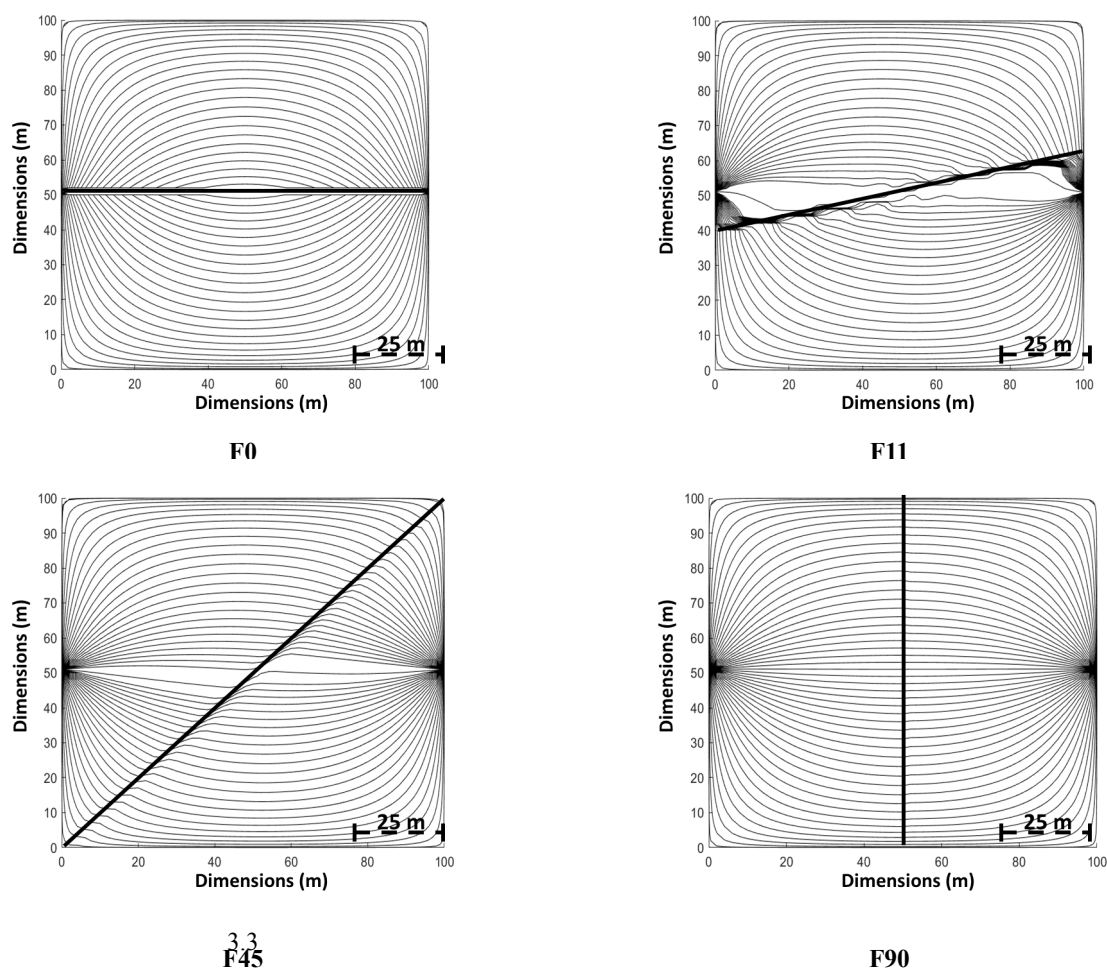
Figure 5: Streamlines for different discontinuity directions. The straight solid line represents the discontinuity location on the model.

4. Discussion

For *F0* (0-degree angle), the pressure magnitude order is two times smaller than the three other cases. However, the pressure for the other 3 cases, 11, 45, and 90 degrees, are in the same order of magnitude. This is because in the case of the 0-degree angle (*F0*), the injector and producer points are located in the discontinuity line and the fluid (here, water) is injected directly in the high permeability discontinuity. In this situation, fluid can flow directly from the injector to the producer with very low resistance against the fluid particles' movement compared to the matrix. This is the main reason that the overall pressure of the model is smaller by almost two orders of magnitude compared to the three other cases. With a constant rate of injection, the pressure goes up if the permeability of the injecting area is not high enough to permeate the injecting fluid. This shows that the choice of injection spot is of great importance. Also, the pore pressure will change the effective stress and can result in instability issues. For *F0* and *F90*, the pressure contours are completely symmetrical, but for *F11* and

F45, there is a slight asymmetrical drift in the contours due to the angle of discontinuity.

A streamline's concentration in a given point represents the amount of flow in that region. This is one of the most useful qualitative data points to focus on in simulating a large scale model. When streamlines get close together, it shows a high flow region. In the DEM-DFN method, which is the most accepted method for simulating a model with discontinuity, the flow trajectories do not represent this kind of information (**Namdari et al. 2016; Zhang, et al., 2002**). In the *F0* case, the streamlines are concentrated on the horizontal line, namely the discontinuity, which shows a high flow region. For *F11*, the difference in concentration is more pronounced, which shows a high-flow zone on the discontinuity. For the *F45* discontinuity, the curve of streamlines changes in the location for *F45*. After that change, streamlines continue to move on a smooth curve to the producer point. For *F90*, there is no change in the streamline's path. This can be explained by the fact that the *F90* model is completely symmetrical with regard to injection and producer points, so the pressure of all of the points
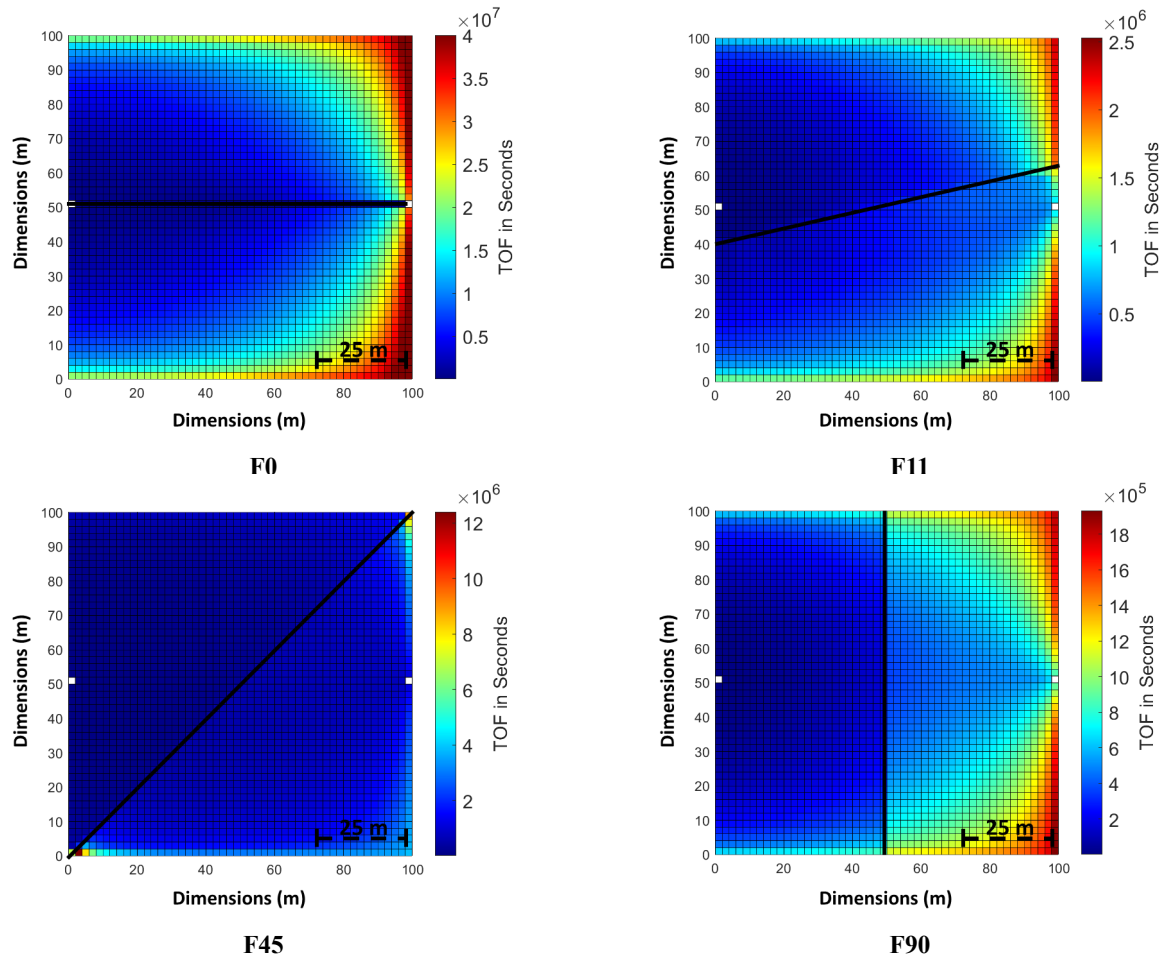
Figure 6: Time Of Flight (TOF) for every model with different discontinuity angles. The blue colour addresses the short time, and the red colour denotes a long time for TOF.

on the discontinuity are equal and there is no hydraulic potential to motivate a flow due to Darcy's law. It can be stated that with an increase in the angle from 0 to 90-degrees of the discontinuity, the impact of the high permeability discontinuity on the streamline's pattern will decrease. For *F0* and *F11*, the impact is very prominent. For *F45,* the change in the streamlines path decreases, and for *F90*, there is no sign of a visual difference in the streamline's path. It can be explained by the fact that for lower angles (e.g., *F0* and *F11*), a great length of the discontinuity is in the direction of the flow (which is in the direction of the pressure gradient or a straight line between the source and sink points) and fluid particles tend to reach to discontinuity to travel faster to the sink point. For higher angles (e.g., *F45*), the angle between the discontinuity and the flow gradient is large, so the discontinuity effects on the streamlines decrease. However, for *F90*, the discontinuity is perpendicular to the pressure gradient, making it impossible for fluid to flow on this direction considering Darcy's law and the direction of the hydraulic gradient from the source to the sink.

In TOF contours, in the *F0* case, the fluid flows very fast on the discontinuity line, and it takes the maximum amount of time for the fluid to access other points on the

matrix because the high permeability on the line segment between the source and the sink is a preferred channel for fluid to flow. For other points of the model, it takes a long time for the fluid to travel from the injector to the producer compared to the other three models. The amount of TOF magnitudes in other locations rather than discontinuity is between 10-100 times larger compared to TOF magnitudes for the same points in the three other models. It is obvious that the presence of the discontinuity makes this bold difference in TOF magnitudes.

With an increase in the discontinuity angle from 0 to 11 degrees, the patterns of TOF contours do not change very much. Since the fluid tends to flow in the lowest resistance path, TOF contours somehow represent the ease of the flow process at a point. If the TOF parameter for a point is low, it is due to the fact that fluid particles reach this point faster than the other points of the model. Hence, time of flight is a relative variable and has to be compared with other points in a model. For *F0, F11* and *F90*, stagnant regions are formed in the upper and lower right corners of the model, whilst the stagnant regions in *F45* are very small compared to other cases and the homogeneity of TOF contours are prominent in the *F45* case. The area of stagnant regions in *F0, F11* and *F90*

are somehow similar, but the TOF magnitudes differ strongly.

This kind of information is lacking in DFN-DEM methods as well, since such methods cannot predict the stagnant regions nor the flowing paths of the fluid particle. Also as mentioned before, the DFN-DEM hybrid models are very slow in terms of running speed that can be from hours to days for a simple dual permeability model. In the used approach in this study, the amount of running time is very small, because this proposed method replaces the discontinuity with porous high permeability cells. So numerous discontinuities can be added to the model without any change in running time.

5. Conclusions

The main challenge in understanding the fluid behaviour in rock masses is to simulate large scale models within a relatively short time in various engineering contexts, like seepage control in underground excavations, geothermal reservoirs and sites of hazardous waste disposal. Different methods have been implemented to investigate the flow pattern in fractured porous rock masses. Many previous studies either consider the fractured medium as an equivalent continuum or simulate the medium with DFN approaches with impermeable rock matrix. In reality, almost every kind of rock has some level of permeability. Using embedded discontinuity in a porous and permeable medium is of great interest in many recent studies. The main problem with these studies is that the simulations need excessive time and computer capacity and each simulation can take hours and even days.

In this study, a novel hybrid FVM-DFN approach is used. The discontinuity is replaced by high permeability cells in different angles of 0, 11, 45, and 90 degrees within a Cartesian network of low permeability limestone matrix of 100×100 m². Using a Two-Point-Flux-Approximation (TPFA) method, fluid injected from the left edge of the model (injector or source point) and produced in the opposite side (producer or sink point). Results are presented through pressure contours, streamlines, and Time Of Flight (TOF) contours. The results show that for *F0* and *F90*, the pressure contours are completely symmetrical, but there is a slight asymmetrical drift in the contours due to the discontinuity's angle. Also, for *F0*, the pressure range in the model is almost two orders of magnitude smaller than the other cases, which can be justified by the fact that injection and production points are on the discontinuity layer and the pressure will be decreased compared to other cases according to Darcy's law. Streamline paths show that for smaller discontinuity angles of *F0* and *F11*, the concentration of streamlines are more prominent due to the fact that the discontinuity is the main channel or flow in these cases. In contrast, for *F45* there is a small bending in a streamline's path. For *F90*, the discontinuity doesn't change the pattern of streamlines, because fluid does not

flow through the discontinuity, due to the fact that the pressures of all of the points on the discontinuity are equal and there is no hydraulic potential to motivate a flow due to Darcy's law.

TOF contours illustrate that for *F0* case, fluid forms stagnated regions in the upper and lower right corners of the model, because the discontinuity is a highly preferred path for flow and in other points of the model, fluid flows slowly and the stagnation initiate. For *F11* and *F90*, stagnant regions are formed in the model's corners, whilst the stagnant regions in *F45* are very small compared to the other cases.

With combining all the contours of pressure, streamlines and TOF, it can be seen that the direction of discontinuity can change the flow regime in DPM rock mass. This is very important in drilling, tunnelling, geothermal reservoir management. These results show that the pressure and flow rate magnitudes are not enough to interpret flow in a rock mass.

From a technical point of view, this study also reveals that runtime has drastically decreased with this hybrid FVM- DFN method in comparison to DFN-DEM approaches. With every run, streamline simulations combined with pressure and TOF contours can provide a detailed insight into the flow pattern of a discrete model with a porous matrix, which can help the engineers in different fields to understand how to operate the projects more efficiently. Also, stagnant regions are hard to detect in DFN-DEM approaches because these approaches break the rock matrix to numerous ultra-small fractures. With these methods and the combination of streamline and TOF contours, the detection of stagnant regions will be straightforward in comparison to other methods.

6. References

Papers:

Baghbanan, A. and Jing, L. (2007): Hydraulic Properties of Fractured Rock Masses with Correlated Fracture Length and Aperture. International Journal of Rock Mechanics and Mining Sciences, 44, 5, 704–719. DOI: 10.1016/j.ijrmms.2006.11.001

Baghbanan, A, Hashemolhosseini, H. and Namdari, S. (2019): 3D Generation of Discrete Fracture Network by Geostatistical Approach, Journal of tunnelling and underground space engineering, 7, 2, 1-28

Batista, D. (2020): Mesh-Independent streamline Tracing. Journal of Computational Physics, 401, 108967, 1-19. DOI: 10.1016/j.jcp.2019.108967

Chen, H., Onishi, T., Olalotiti-Lawal, F., and Datta-Gupta, A. (2020): Streamline tracing and applications in embedded

discrete fracture models. Journal of Petroleum Science and Engineering, 188, 106865, 1-20. DOI: 10.1016/j.petrol.2019.106865

Dailami, K., Nasriani, H.R., Sajjadi, S.A., Rafiee, M.R., Whitty, J. and Francis, J. (2020): Optimizing the ultimate recovery by infill drilling using streamline simulation. Acta Scientiarum Technology, 42, 1, 1-9. DOI: 10.4025/actascitechnol.v42i1.45293

Habibi, M.J., Mokhtari, A.R., Baghbanan, A. and Namdari, S. (2014): Prediction of permeability in dual fracture media by multivariate regression analysis. Journal of Petroleum Science and Engineering, 120, 194–201. DOI: 10.1016/j.petrol.2014.06.016

Huang, F., Yao, C., Zhang, X., Wu, L., Shao, Y. and Zhou, C. (2021a): Effects of fracture parameters and roughness on heat-flow coupling in rock masses with two-dimensional fracture networks. Energy Science & Engineering. 00, 1-16. DOI: 10.1002/ese3.885

Huang, N., Liu, R., Jiang, Y. and Cheng, Y. (2021b): Development and application of three-dimensional discrete fracture network modelling approach for fluid flow in fractured rock masses. Journal of Natural Gas Science and Engineering, 91, 103957. DOI: 10.1016/j.jngse.2021.103957

Karimzade, E., Sharifzadeh, M., Zarei, H.R., Shahriar, K. and Seifabad, M.C. (2017): Prediction of water inflow into underground excavations in fractured rocks using a 3D discrete fracture network (DFN) model. Arabian Journal of Geosciences, 10, 206, 1-14. DOI: 10.1007/s12517-017-2987-z

Li, X., Li, D., Xu, Y. and Feng, X. (2020): A DFN based 3D numerical approach for modelling coupled groundwater flow and solute transport in fractured rock mass. International Journal of Heat and Mass Transfer, 149, 119179, 1-15. DOI: 10.1016/j.ijheatmasstransfer.2019.119179

Macenić, M., Kurevija, T. and Strpić, K. (2018): Systematic review of research and utilization of shallow geothermal energy in Croatia. Rudarsko-Geološko-Naftni Zbornik, 43, 5, 1-11. DOI: 10.17794/rgn.2018.5.4

Namdari, S., Baghbanan, A. and Habibi, M.J. (2016): Effects of matrix permeability and fracture density on flow pattern in dual porous rock masses. Paper presented at the ISRM International Symposium - EUROCK 2016, Ürgüp, Turkey, August 2016. Paper Number: ISRM-EUROCK-2016-087, 10-14

Namdari, S., Habibi, M.J. and Baghbanan, A. (2012): A comparison between permeability of single porosity and dual porosity medium using DFN and Dual fracture method (DFM). Paper presented at the ISRM International Symposium - EUROCK 2012, 2012 ISRM international symposium, 28-30 May 2012, Stockholm, Sweden. Paper Number: ISRM-EUROCK-2012-130, 101-110

Neuman, S.P. (2005): Trends, prospects and challenges in quantifying flow and transport through fractured rocks. Hydrogeology Journal, 13, 1, 124–147. DOI: 10.1007/s10040-004-0397-2

Nunes, J.P.P., Bijeljic, B. and Blunt, M.J. (2015): time-of-flight distributions and breakthrough curves in heterogeneous porous media using a pore-scale streamline tracing algorithm. Transport in Porous Media, 109, 2, 317–336. DOI: 10.1007/s11242-015-0520-y

Odling, N.E. and Roden, J.E. (1997): Contaminant transport in fractured rocks with significant matrix permeability, using natural fracture geometries. Journal of Contaminant Hydrology, 27, 263–283. DOI: 10.1016/S0169-7722(96)00096-4

Ooriad, F.A., Yari, M., Bagherpour, R. and Khoshouei, M. (2018): The development of a novel model for mining method selection in a fuzzy environment; case study: Tazareh Coal Mine, Semnan Province, Iran. Rudarsko-Geološko-Naftni Zbornik, 33, 1, 45–53. DOI: 10.17794/rgn.2018.1.6

Pašić, B., Gaurina Međimurec, N. and Matanović, D. (2007): Wellbore instability: causes and consequences. Rudarsko-Geološko-Naftni Zbornik, 19, 1, 87–98.

Ren, F., Ma, G., Fan, L., Wang, Y. and Zhu, H. (2017): Equivalent discrete fracture networks for modelling fluid flow in highly fractured rock mass. Engineering Geology, 229, 21–30. DOI: 10.1016/j.enggeo.2017.09.013

Ružičić, S., Mileusnić, M. and Posavec, K. (2012): Building conceptual and mathematical model for water flow and solute transport in the unsaturated zone at Kosnica site. Rudarsko-Geološko-Naftni Zbornik, 25, 1, 21–31.

Seales, M.B. (2020): Multiphase Flow in Highly Fractured Shale Gas Reservoirs: Review of Fundamental Concepts for Numerical Simulation. Journal of Energy Resources Technology, 142, 10, 1-66. DOI: 10.1115/1.4046792

Siavashi, M., Blunt, M.J., Raisee, M. and Pourafshary, P. (2014): Three-dimensional streamline-based simulation of non-isothermal two-phase flow in heterogeneous porous media. Computers & Fluids, 103, 116–131. DOI: 10.1016/j.compfluid.2014.07.014

Sokolova, I., Bastisya, M.G. and Hajibeygi, H. (2019): Multiscale finite volume method for finite-volume-based simulation of poroelasticity. Journal of Computational Physics, 379, 309–324. DOI: 10.1016/j.jcp.2018.11.039

Sun, Z., Jiang, C., Wang, X., Lei, Q. and Jourde, H. (2020): Joint influence of in-situ stress and fracture network geometry on heat transfer in fractured geothermal reservoirs. International Journal of Heat and Mass Transfer, 149, 119216, 1-21. DOI: 10.1016/j.ijheatmasstransfer.2019.119216

Thiele, M.R. and Batycky, R.P. (2006): Using streamline-derived injection efficiencies for improved waterflood management. SPE Reservoir Evaluation & Engineering, 9, 02, 187–196. DOI: 10.2118/84080-PA

Wang, L., Zuo, L. and Zhu, C. (2020): Tracer Test and Streamline Simulation for Geothermal Resources in Cuona of Tibet. Fluids, 5, 3, 1-14. DOI: 10.3390/fluids5030128

Wang, W., Fan, D., Sheng, G., Chen, Z. and Su, Y. (2019): A review of analytical and semi-analytical fluid flow models for ultra-tight hydrocarbon reservoirs. Fuel, 256, 115737, 1-17. DOI: 10.1016/j.fuel.2019.115737

Zhang, F., Damjanac, B. and Maxwell, S. (2019): Investigating hydraulic fracturing complexity in naturally fractured rock masses using fully coupled multiscale numerical modelling. Rock Mechanics and Rock Engineering, 52, 12, 137–160. DOI: 10.1007/s00603-019-01851-3

Zhang, N., Cao, J., James, L.A. and Johansen, T.E. (2021): High-order Streamline Simulation and Macro-scale Visualization Experimental Studies on Waterflooding under given Pressure Boundaries. Journal of Petroleum Science and Engineering, 203, 108617. DOI: 10.1016/j.petrol.2021.108617

Zhang, X., Sanderson, D.J. and Barker, A.J. (2002): Numerical study of fluid flow of deforming fractured rocks using dual permeability model. Geophysical Journal International, 151, 2, 452–468. DOI: 10.1046/j.1365-246X.2002.01765.x

Books/thesis:

Baghbanan, A. (2008): Scale and Stress Effects on Hydro-Mechanical Properties of Fractured Rock Masses. PhD thesis in engineering geology and geophysics research group. . Royal Institute of Technology (KTH). 91 p.

Bear, J., Tsang, C.F. and De Marsily, G. (1993): Flow and Contaminant Transport in Fractured Rock. Academic Press. 560 p.

Datta-Gupta, A., and King, M.J.. (2007): Streamline Simulation: Theory and Practice. Society of Petroleum Engineers. SPE textbook series Vol . 11. 404 p.

Jing, L. and Stephansson, O. (2007): Fundamentals of Discrete Element Methods for Rock Engineering. Developments in Geotechnical Engineering, vol. 85. 450 p.

Lie, K.A. (2019): An introduction to reservoir simulation using MATLAB/GNU Octave: User guide for the MATLAB Reservoir Simulation Toolbox (MRST). Cambridge University Press. 678 p.

Moukalled, F., Mangani, L. and Darwish, M. (2016): The finite volume method in computational fluid dynamics (Vol. 113). Springer publ. Co., 1164 p.

Olu-Ojo, T. (2020): Permeability Evolution in Sandstone and Carbonate after Fracture Induced by CO2 Injection. Curtin University publ. 85 p.

Zhang, X. and Sanderson, D.J. (2002): Numerical modelling and analysis of fluid flow and deformation of fractured rock masses. Elsevier publ., 300 p.

Chapters in books or proceedings with editor(s):

Jing, L., and Stephansson, O. (2007): The Basics of Fracture System Characterization–Field Mapping and Stochastic Simulations. In Jing, L., and Stephansson, O.: Fundamentals of discrete element method for rock engineering. Developments in Geotechnical Engineering, vol. 85, 147–177, 450 p.

Chillingar, G.V., Bissell, H.J. and Wolf, K.H. (1979): The Diagenesis of Carbonate Sediments and Epigenesis (or Catagenesis) of Limestone. In: Larsen, G. and Chillingar, G.V. (eds.): Diagenesis in Sediments and Sedimentary Rocks. – Elsevier Publ. Co., 247-422, 579 p.

SAŽETAK

Ispitivanje utjecaja pružanja diskontinuiteta na regionalni protok fluida u šupljikavoj stijeni uporabom hibridne metode konačnih volumena i mreže diskretnih pukotina te simulacijom strujnica

Razumijevanje ponašanja fluida u stijenskoj masi izrazito je važno kod različitih inženjerskih projekata kao što su procjeđivanje u tunelima, geotermalna ležišta te odlaganje opasnoga otpada. U proučavanju obrasca protoka fluida kroz raspucanu, šupljikavu stijensku masu korišteni su različiti pristupi. Laboratorijska istraživanja mogu pomoći u izučavanju takvih problema, međutim, osim što su skupa, zahtijevaju puno vremena i teško ih je primijeniti u makrostrukturama. Numeričke simulacije mogu opisati takve prostore metodom mreže diskretnih pukotina smanjujući troškove i vrijeme jer nude dovoljnu prilagodljivost i kreativnost. Ovdje je prikazano proširenje koda u Matlabu s ciljem izučavanja protoka u stijenskome prostoru s dvostrukom propusnošću, tj. s izvorima fluida na desnoj i lijevoj strani modela koji predstavljaju utisnu i proizvodnu bušotinu. Vrlo propusni diskontinuiteti s različitim kutovima smješteni su unutar slabopropusnoga vapnenačkog matriksa. Jednadžbe tlaka aproksimiraju izravan shematski tok između dviju točaka metodom konačnih volumena. Strujnice su praćene kroz simulirani volumen te je njima analizirano hidrauličko ponašanje modela izračunom brzine protoka u svakoj točki. Rezultati pokazuju kako hibridna metoda konačnih volumena i mreža diskretnih pukotina mogu biti korištene kao brz način opisivanja protoka fluida u prostoru s dvostrukom propusnošću, tj. uz pomoć simulacije strujnica unutar makromodela s diskontinuitetima.

Ključne riječi:
simulacija strujnica, prostor dvostruke poroznosti, aproksimacija toka s dvjema točkama, hibridne metode

Author's contribution

Sajad Namdari (Ph.D. student in rock mechanics) extended a computer code and presented the results with analysis. **Alireza Baghbanan** (associate professor) provided the analyses and point of view. **Hamid Hashelolhosseini** (Associate professor) provided the mathematical fundamentals.